Optical and Electrical Investigations on GaAs-Based Phototransistors

Sven Bader and Andreas Ziegler

In order to exploit the potential of phototransistors for vertical-cavity surface-emitting laser (VCSEL) applications, optical and electrical investigations on GaAs-based devices were conducted. The characterization of phototransistors consists of measurements and improvements of the current gain and studies on the spectral behavior. In addition, the influences of various doping concentrations and different device structures, such as resonant-cavity-enhanced phototransistors, will be introduced and discussed.

1. Introduction

The detection of infrared signals in optical fiber communication is one of the most quoted applications for phototransistors [1]. High optical gain without excess noise is a potential advantage over the competitive device, the avalanche photodiode [2]. Phototransistors combine the functions of photodiodes and bipolar transistors. Hence, the structure of the device is similar to a common npn- or pnp-bipolar transistor, which consists of emitter, base and collector layers. In this article, we investigate exclusively the pnp structure. To achieve high current gain, it is necessary to integrate a heterojunction, thus a potential barrier, between the p-emitter and n-base layers, equivalent to a heterojunction bipolar transistor (HBT). According to this, the device is similarly named heterojunction phototansistor (HPT). With an HPT it is possible to reach current gains between 10^2 and 10^5 [3]. The photodetection occurs in the depletion zone of the n-base and p-collector junction due to the photoeffect. In more special cases, there is a separate absorption layer with defined width d and absorption coefficient α embedded between the two layers. Incident photons with a total power P_0 and wavelength λ are absorbed and generate the photocurrent I_{ph}, which is equivalent to the base current I_{B} and can be calculated accordingly as

$$I_{\mathrm{B}} \mathrel{\hat{=}} I_{\mathrm{ph}} = (1-R) \cdot (1-\exp(-\alpha d)) \cdot \frac{q\lambda}{hc} \cdot P_0\,. \tag{1}$$

R is the intensity reflection coefficient of the surface due to the refractive index step from air to semiconductor, q the elementary charge, h is Planck's constant, and c the vacuum velocity of light. Thus, no external base current is necessary. In active operation, the applied voltage U_{EC} between the emitter and collector layers should be positive. Hence, the electrons of the photocurrent are swept directly through the n-doped base towards the p-emitter layer, where the integrated heterojunction blocks the majority of these free carriers to prevent them from recombining with the holes. Due to the charge neutrality of the base, this leads to an injection of holes into the base layer, the so-called collector

hole current I_{C} [4]. The ratio between the collector and base current is defined as current gain [5]

$$\beta = I_{\mathrm{C}}/I_{\mathrm{B}}. \tag{2}$$

High current gain requires $w_{\mathrm{B}} \ll L_{\mathrm{D}}$, where w_{B} is the width of the base and L_{D} represents the diffusion length of the holes in the n-base. Otherwise, the recombination in the base would decrease I_{C} and hence the current gain dramatically. Moreover, w_{B} should not be chosen too thin. This would lead to an early breakdown of the device at low U_{EC}, where the collector current rises exponentially. This occurs when both depletion zones, namely of the emitter–base and base–collector junctions, touch before current-mode operation (where I_{C} is quasi independent of U_{EC}) could be reached. The breakdown voltage can be adjusted by a proper choice of the doping concentrations of the base $N_{\mathrm{n,B}}$ and the collector $N_{\mathrm{p,C}}$. Therefore, for common devices, $N_{\mathrm{n,B}} > N_{\mathrm{p,C}}$ should be valid. As a result, the base–collector depletion zone spreads almost completely into the collector region. Normally, it also makes sense to dope the emitter more than the base ($N_{\mathrm{p,E}} > N_{\mathrm{n,B}}$), which limits the recombination current at the emitter–base junction. However, due to the integrated potential barrier at the interface, this requirement can be neglected.

2. Experimental

To investigate fabricated GaAs-based HPTs with respect to their output characteristics, breakdown voltage, current gain, and spectral absorption behavior, the measurement setup shown in Fig. 1 (left) is used. Light emitted from a VCSEL with defined wavelength is collimated and focused on an HPT. The intensity of the light can be adjusted by the current source in the circuit. U_{EC} is delivered by a controllable voltage source with integrated amperemeter to measure the collector current I_{C}. For spectral studies, the wavelength can be changed by replacing the VCSEL device. Four different wavelengths are available here, namely 980, 995, 1040, and 1130 nm. For refined measurements, a monochromator with external lock-in amplifier was used for illumination. Figure 1 (right) shows the schematic layer structure of the HPT, grown by molecular beam epitaxy (MBE). Above the GaAs substrate, the p-doped collector encloses the InGaAs absorption layer with the n-doped base. The absorption layer consists of a 5 nm thick quantum well (QW), which is embedded between two undoped GaAs barrier layers to guarantee intrinsic characteristics. The emitter layer on top of the HPT stack consists of two equally p-doped layers of GaAs and AlGaAs, forming the required heterojunction. To contact the HPT electrically, Ti/Pt/Au top and bottom contacts are evaporated.

2.1 Output characteristics

Calculations of the current gain by (2) require investigations on the output characteristics of the transistor. First measurements of the grown HPT, represented in Fig. 2 (left), show no perceivable current-source mode and only small collector currents in the low µA-range for vanishing optical input powers P. As expected, with increasing P at $\lambda = 980$ nm, I_{C} raises slightly because of the higher amount of absorbed photons. This HPT does not

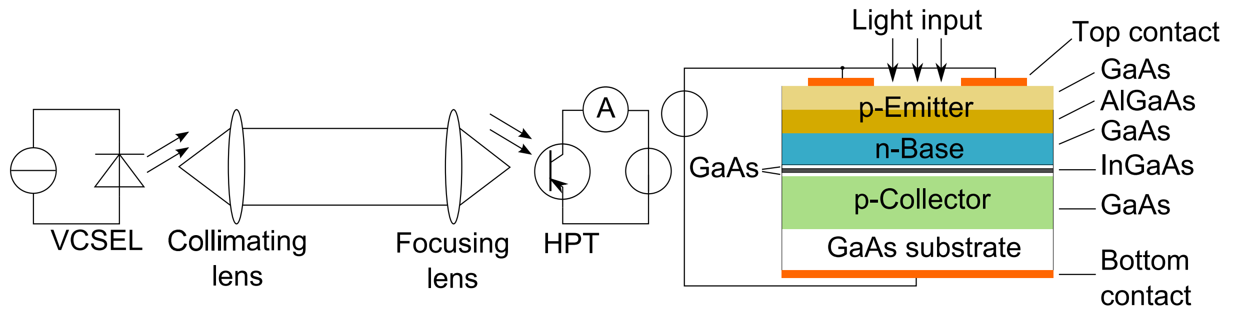

Fig. 1: Measurement setup for optoelectronic investigations on HPTs (left) and schematic layer structure of the GaAs-based HPT (right).

exhibit any current confinement. In consequence, the collector current spreads laterally over the wafer sample and is influenced by the sheet resistance. To force the current to propagate directly through the device and thus reduce lateral leakage currents, a mesa was wet-chemically etched. The output characteristics of the mesa-etched device are shown in Fig. 2 (right). Increasing U_{EC}, three operating regions can clearly be distinguished: The saturation region, the current-source mode, and the breakdown region. The saturation region occurs at low U_{EC} when both pn-junctions, namely of the emitter–base and base–collector, are biased in forward direction. However, the magnitude of the collector current is also decreased, probably due to surface leakage currents along the mesa walls.

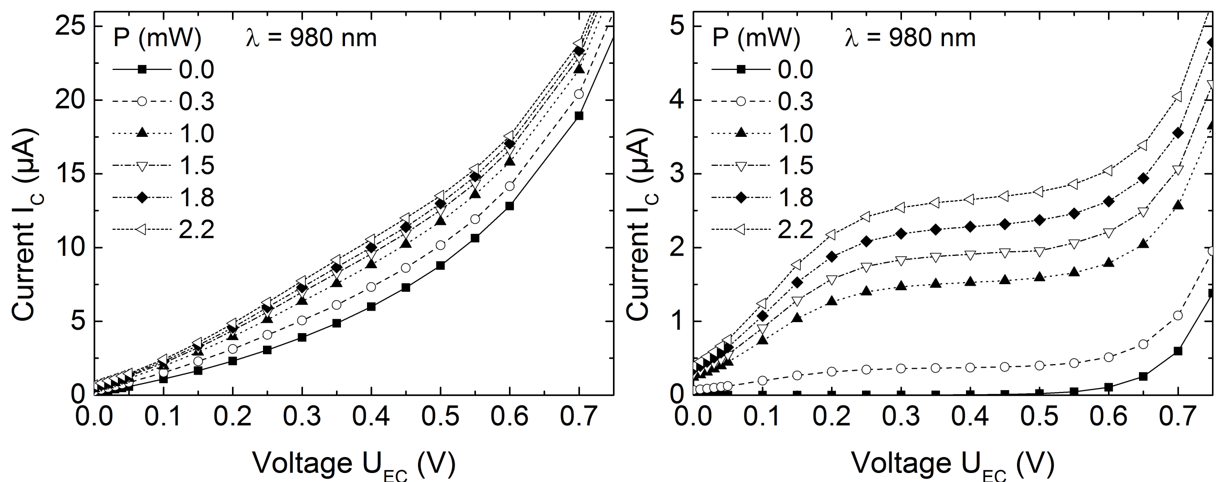

Fig. 2: Measured output characteristics of planar (left) and mesa-etched HPTs using a 980 nm VCSEL for illumination (right).

Calculations of the current gain applying (1) and (2) result in $\beta \approx 1$. This behavior is known and well explained in the literature using the so-called Gummel plot [6]. Low collector currents result in low current gains due to high recombination currents in the emitter–base depletion zone and surface and interface leakage currents. To minimize these effects, the collector current must be increased. This can be solved easily by raising the incident optical power or by ensuring more efficient light absorption.

2.2 Resonant-cavity-enhanced phototransistors

The VCSEL output power cannot be increased arbitrarily because of thermal roll-over. Hence, the light intensity must be increased in a different way. Therefore, the HPT is embedded between two Bragg reflectors, as seen in Fig. 3 (left), to form a resonant cavity. The top Bragg reflector has a reflectivity of $R_t \approx 0.7$, whereas $R_b \approx 1$ for the bottom mirror. The resonant cavity raises the probability of a photon to be absorbed by the InGaAs QW by a factor of $M \approx 2/(1 - R_t R_b) \approx 6.7$, where $M/2$ represents the effective number of round-trips of the photon in the resonator. Hence, the quantum efficiency is strongly increased [2]. Measurements of the reflection spectrum of the device clearly show a resonance dip at 1040 nm, which requires using a VCSEL with similar wavelength for external illumination.

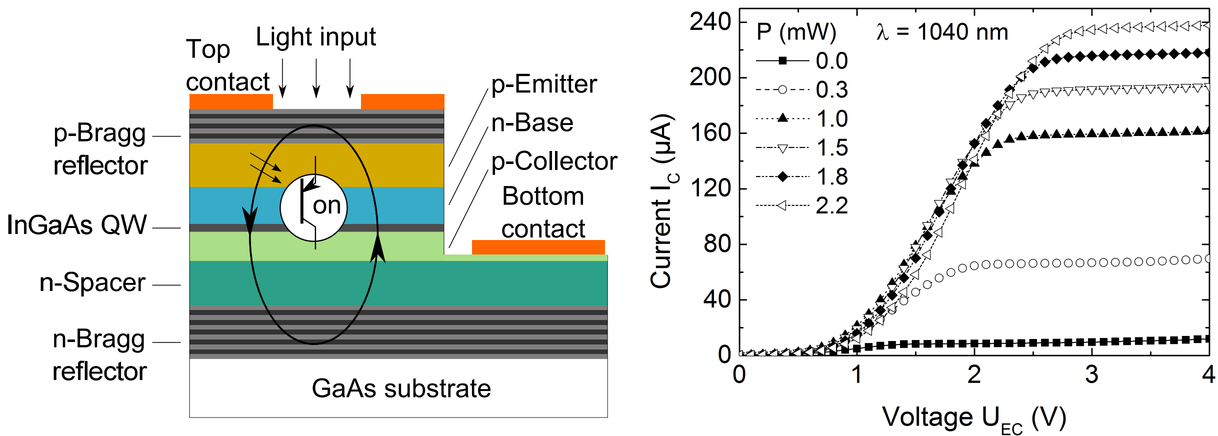

Fig. 3: Schematic layer structure of a resonant-cavity-enhanced phototransistor (left) and measured output characteristic with an incident photon wavelength of 1040 nm (right).

Figure 3 (right) depicts the results of the measured output characteristics. Qwing to a decreased collector doping concentration in comparison to the HPT of Sect. 2.1, the breakdown voltage has raised up to ≈ 7 V. The collector current now reaches 240 µA for an incident optical power of 2.2 mW. Compared to the results seen in Fig. 2 (right), the collector current has increased almost by a factor of 80. Taking the increased quantum efficiency of the resonant cavity into account, the calculated current gain of the HPT is $\beta \approx 165$. This proves the functionality of the phototransistor and confirms the theory of the Gummel plot.

2.3 Spectral investigations

As described in the introduction of Sect. 2, the InGaAs QW is responsible for the absorption of the incident photons. To adjust the wavelength sensitivity of the HPT, it is necessary to do spectral investigations of the absorption coefficient of the QW. As a first step, we have measured the output characteristics of the HPT using the above mentioned four VCSELs with different wavelengths (Fig. 4 (left)). The bandgap wavelengths λ_g of GaAs and the AlGaAs material in the HPT amount to 875 nm and 722 nm, respectively,

which means that the material is transparent when using the 980 nm VCSEL. The target λ_g of the $In_{0.27}Ga_{0.73}As$ QW absorbing layer is 1074 nm. At $\lambda = 1130$ nm the curve is similar to the dark current. Because of the low energy of the photons, absorption in the InGaAs QW is not possible, in contrast to measurements using the 1040 nm VCSEL. Hence, the bandgap wavelength of the QW could be estimated to $1040\,\text{nm} \leq \lambda_g \leq 1130\,\text{nm}$. A further decrease of the photon wavelength results in a slight increase of the collector current.

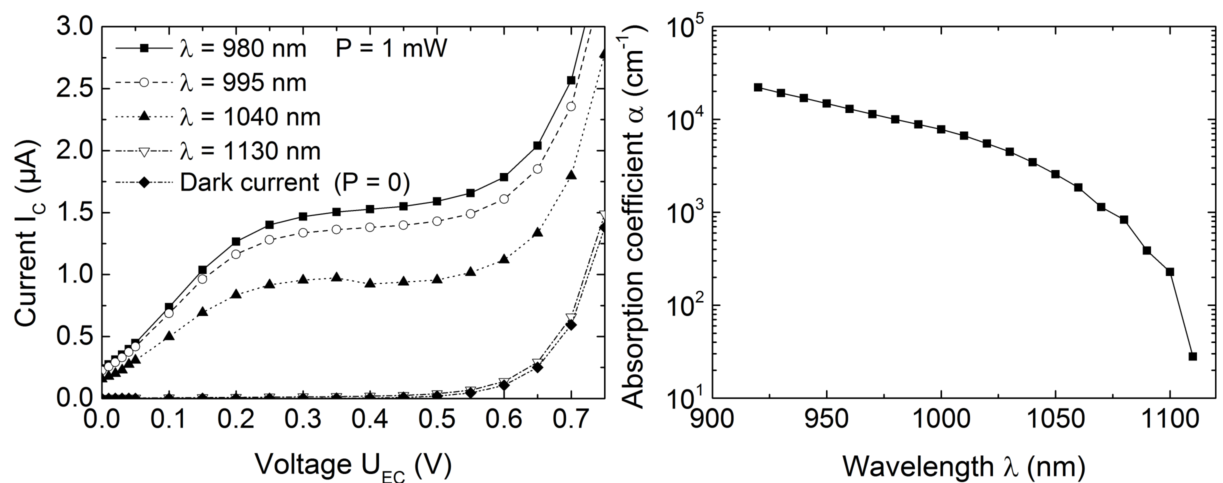

Fig. 4: HPT output characteristics for four different VCSEL wavelengths at an optical power of 1 mW (left) and measured spectral absorption coefficient of an $In_{0.27}Ga_{0.73}As$ QW using a monochromator (right).

More accurate measurements were possible by substituting the VCSEL by a halogen lamp and a monochromator. The low spectral power density required the use of a lock-in amplifier. Assuming an absorption coefficient of $\alpha = 10^4\,\text{cm}^{-1}$ at $\lambda = 980$ nm, the wavelength-dependent absorption coefficient can be calculated using (2) and (1), as shown in Fig. 4 (right). There is a strong drop of α towards long wavelengths (note the logarithmic scale), however, a band edge wavelength cannot be easily identified. As an estimation, $1070\,\text{nm} \leq \lambda_g \leq 1100\,\text{nm}$. This interval includes the design λ_g of the QW.

3. Conclusion

We have investigated heterojunction phototransistors in order to achieve high current gain and to determine the spectral absorption coefficient of the InGaAs QW absorbing layer in the collector–base depletion zone. We have shown the advantages of mesa-etched structures and have reached high current gain using a resonant-cavity-enhanced HPT, in which the absorption probability of the photons is increased. Although the experimental absorption spectrum shows a more gradual decrease towards the band edge than expected, λ_g can be estimated and is in good agreement with the target bandgap wavelength.

Acknowledgment

We thank Philips Technologie GmbH (U-L-M Photonics) for the MBE growth of the phototransistors and Dr.-Ing. Philipp Gerlach for supplying the transistor and laser samples as well as numerous and fruitful discussions. Also we acknowledge the technical contributions of Rudolf Rösch.

References

[1] R.A. Milano, P.D. Dapkus, and G.E. Stillman, "An analysis of the performance of heterojunction phototransistors for fiber optic communications", *IEEE Trans. Electron Dev.*, vol. 29, pp. 266–274, 1982.

[2] M.S. Ünlü, K. Kishino, J.-I. Chyi, L. Arsenault, J. Reed, S.N. Mohammad, and H. Morkoç, "Resonant cavity enhanced AlGaAs/GaAs heterojunction phototransistors with an intermediate InGaAs layer in the collector", *Appl. Phys. Lett.*, vol. 57, pp. 750–752, 1990.

[3] F. Träger, *Springer Handbook of Lasers and Optics.* Berlin: Springer, 2012.

[4] N. Chand, P.A. Houston, and P.N. Robson, "Gain of a heterojunction bipolar phototransistor", *IEEE Trans. Electron Dev.*, vol. 32, pp. 622–627, 1985.

[5] N. Pan, J. Elliott, M. Knowles, D.P. Vu, K. Kishimoto, J.K. Twynam, H. Sato, M.T. Fresina, and G.E. Stillman, "High reliability InGaP/GaAs HBT", *IEEE Electron Dev. Lett.*, vol. 19, pp. 115–117, 1998.

[6] S.M. Sze, *Physics of Semiconductor Devices.* New York: John Wiley and Sons, 1981.